

Original article

# Histology and growth pattern of the pachy-osteosclerotic premaxillae of the fossil beaked whale *Aporotus recurvirostris* (Mammalia, Cetacea, Odontoceti)<sup>☆</sup>

*Histologie et mode de croissance des prémaxillaires hyperplasiques du Ziphidae fossile Aporotus recurvirostris (Mammalia, Cetacea, Odontoceti)*

Vivian de Buffrénil <sup>a,\*</sup>, Olivier Lambert <sup>a,b</sup>

<sup>a</sup> UMR 7207 (CR 2P), département Histoire de la Terre, Muséum national d'Histoire naturelle, 8, rue Buffon, 75005 Paris, France

<sup>b</sup> Département de paléontologie, Institut royal des Sciences naturelles de Belgique, rue Vautier, 1000 Brussels, Belgium

Received 22 March 2010; accepted 21 September 2010

Available online 23 December 2010

---

## Abstract

Beaked whales (Ziphidae) often show highly specialized features, involving bone morphology or structure, in the rostral region of their skulls. Previous studies revealed an extremely derived and peculiar histological structure in the rostrum of the extant *Mesoplodon densirostris*. In order to assess if this structure is a general feature of ziphids, the swollen premaxillae of *Aporotus recurvirostris*, a Miocene species from the North Sea, were studied histologically. These bones are pachyostotic and strongly osteosclerotic. However, their structural organization is entirely different from that of *M. densirostris* rostrum: they are basically made of a non-remodeled, laminar tissue that was cyclically deposited by the periosteum. As compared to the generalized structure of the premaxillae of toothed whales exemplified by the bottlenose dolphin, *Tursiops truncatus*, the pachyostotic condition of *Aporotus* premaxillae was obviously due to a particularly high and sustained growth-rate, occurring in a dorso-lateral direction. The osteosclerotic structure of these bones resulted from a complete lack of inner resorption activity. The histological features of *Aporotus* premaxillae indicate that these bones are not likely to have been hypermineralized, and thus, their physical properties must have differed from those of the *M. densirostris* rostrum. The possible functional involvements of rostral peculiarities in beaked whales are discussed with reference to the whole set of available comparative data.

© 2011 Elsevier Masson SAS. All rights reserved.

**Keywords:** Ziphidae; Bone; Histology; Growth; Rostrum; Functional interpretation

## Résumé

La région rostrale du crâne des baleines à bec (Ziphidae) montre souvent des caractères très spécialisés, touchant la morphologie ou la structure des os. Les études précédentes ont mis en évidence une organisation histologique extrêmement dérivée et particulière des os du rostre de l'espèce actuelle *Mesoplodon densirostris*. Dans le but de vérifier si cette structure est un caractère général chez les Ziphidae, l'histologie des prémaxillaires fortement saillants et boursouflés d'*Aporotus recurvirostris*, une espèce du Miocène de la Mer du Nord, a été examinée. Ces os sont pachyostotiques et ostéosclérotiques. Cependant, leur organisation structurale diffère totalement de ce que montre le rostre de *M. densirostris* : ils sont formés d'un tissu laminaire non remanié, déposé par le périoste sur un mode cyclique. Par comparaison avec la structure généralisée des prémaxillaires des odontocètes, telle qu'elle apparaît chez *Tursiops truncatus*, la pachyostose des prémaxillaires d'*Aporotus* paraît avoir résulté d'une vitesse de croissance particulièrement élevée et soutenue, se produisant en direction dorso-latérale. L'ostéosclérose de ces os était due à une absence complète de résorption interne. Les caractères histologiques des prémaxillaires d'*Aporotus* suggèrent que ces os n'étaient pas hyperminéralisés et que, par conséquent, leurs propriétés physiques différaient de celles du rostre de *M. densirostris*. L'implication fonctionnelle des particularités que montre le rostre des baleines à bec est discutée en référence à l'ensemble des données comparatives actuellement disponibles.

© 2011 Elsevier Masson SAS. Tous droits réservés.

**Mots clés :** Ziphidae ; Os ; Histologie ; Croissance ; Rostre ; Interprétation fonctionnelle

---

<sup>☆</sup> Corresponding editor: Gilles Escarguel.

\* Corresponding author.

E-mail address: vdebuff@mnhn.fr (V. de Buffrénil).

## 1. Introduction

The skeletons of tetrapods secondarily adapted to life in water display various specialized features involving both the gross morphology, and the internal structure of bones (reviewed by Ricqlès and Buffrénil, 2001). One of the most extreme structural specializations occurs in the facial complex of some toothed whales (Odontoceti), especially the beaked whales

(Ziphidae). In the extant beaked whale *Mesoplodon densirostris*, the rostral region of adult males (this region includes the maxillae, premaxillae, vomer, palatines and pterygoids *pro parte*) is composed of the densest, hardest, most compact, and most mineralized osseous tissue ever described in a vertebrate (Buffrénil and Casinos, 1995; Zioupos et al., 1997). Such characteristics appear during the remodeling process of the bones. They result from a structural modification and a steep

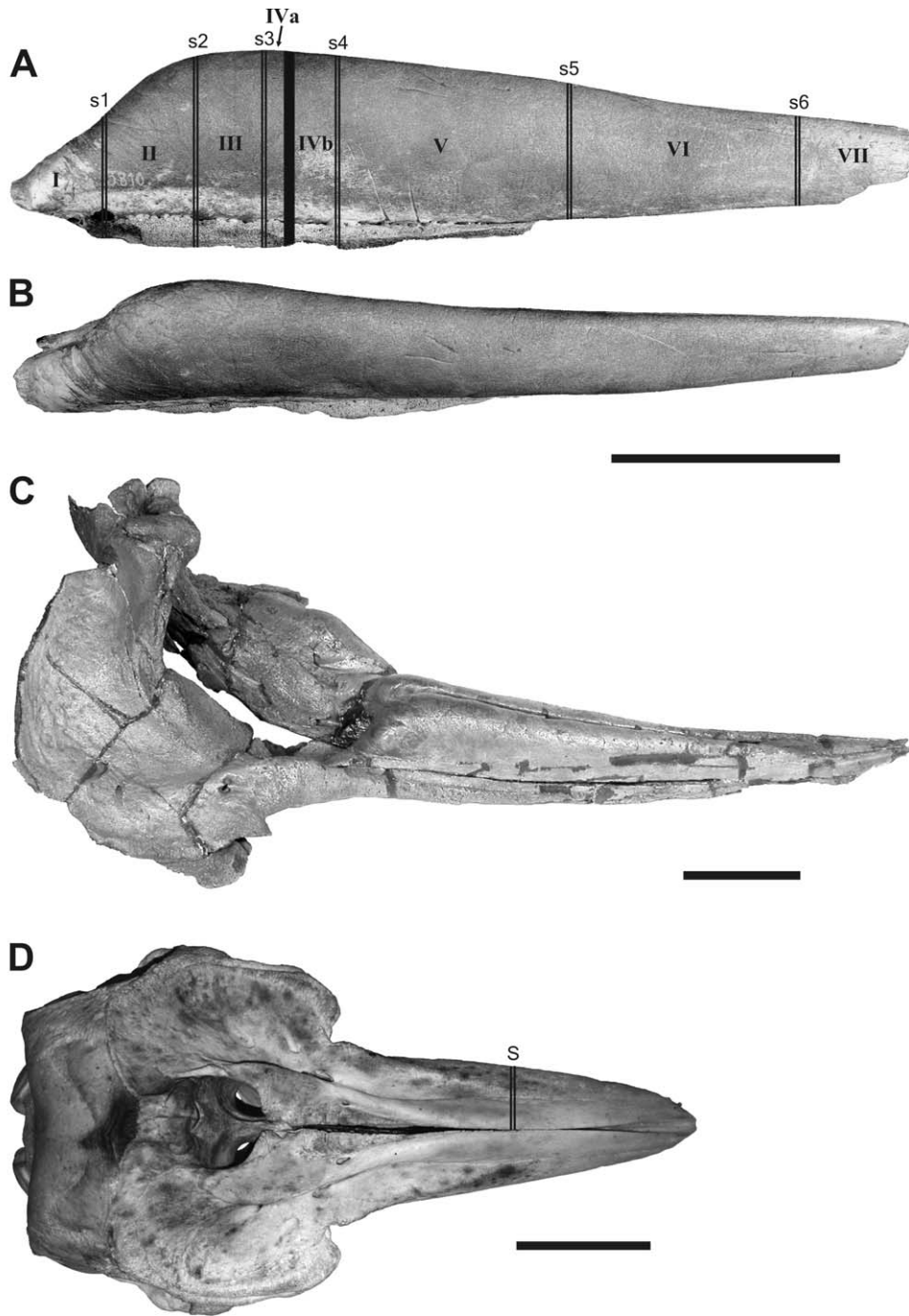


Fig. 1. General morphology of the premaxilla IRSNB 3810-M. 2012 a-b used in this study. **A.** Right lateral view. **B.** Dorsal view. **C.** General aspect of the skull (represented by face bones only) of the holotype of *Aporotus recurvirostris* (specimen IRSNB M.1887) in right dorso-lateral view (modified from Lambert, 2005). **D.** Dorsal view of *Tursiops truncatus* skull, with indication of the section(s) made in the rostrum. The Roman numbers I–VII designate the seven segments sampled from the bone of *Aporotus recurvirostris*; s1 to s6: location and orientation of the six ground sections made in the bone fragments. The thick bar between IVa and IVb localizes the preliminary section. Scale bars = 10 cm.

decrease in volume of the collagenic component of bone matrix, with a consecutive increase in bone mineralization (Zylberberg et al., 1998; Buffrénil et al., 2000). Up to now, there is no clear, unequivocal interpretation of the functional role, or adaptive value, of these features (Heyning, 1984; Ziopoulos et al., 1997; MacLeod, 2002).

Other ziphids display remarkable peculiarities of the rostral region, generally resulting in a spectacular increase in local bone volume and/or compactness. The study of these taxa could thus contribute to further documenting the osteogenic processes, and adaptive context, involved in the development of such peculiar morphological traits. One of the most obvious cases is encountered in *Aporotus* du Bus, 1868, from the Miocene of the southern margin of the North Sea, Antwerp region, Belgium. This taxon is member of an unnamed clade of fossil beaked whales (together with, e.g., *Beneziphius*, *Choneziphius*, *Messapicetus*, and *Ziphirostrum*) displaying a dorsal hump of the premaxillae that is variably pronounced among taxa and unknown in other toothed whales (Lambert, 2005; Bianucci et al., 2010). This trend reaches a peak in *Aporotus recurvirostris* and, to a lesser extent, *Aporotus dicyrtus*, the premaxillae of which project upwards into strong bulbous crests that meet (without fusing) along the mid-sagittal plane of the rostrum, and increase considerably the volume of these bones. Up to now, the inner osseous structure to which this singular morphology is associated, as well as the growth processes from which it results, are unknown. As a consequence, it is neither possible to assess the degree of convergence that this feature shares with the compaction of face bones in *Mesoplodon densirostris*, nor to know if there is, in the Ziphidae, a true homology (that could rank as a synapomorphy) in the local osteogenic processes involved in the creation of the specialized structural features of the rostrum.

The present article describes the structural organization of *A. recurvirostris* premaxillae, and proposes an interpretation for the growth pattern of these bones.

## 2. Material and methods

### 2.1. *Aporotus recurvirostris* sample

The paleontological material consists of the rostral portion of a right premaxilla (Fig. 1(A, B)) of *Aporotus recurvirostris* du Bus, 1868, from the collections of the Institut royal des sciences naturelles de Belgique, Brussels (IRSNB) where it is recorded under the reference IRSNB 3810-M. 2012 a-b. In 2008, this bone had been cut transversely into two pieces 271 and 121 mm long, respectively (which explains the letters “a” and “b” in its reference) for a preliminary view of its inner structure. Before section, this bone measured 395 mm, from the premaxillary foramen to the broken anterior tip (80–100 mm missing). Small remnants of the right maxilla still adhere to the ventral margin of the premaxilla. The maximal height of our fossil is 87.74 mm, in which 11.05 mm correspond to the maxilla, and 76.69 mm to the premaxilla. The length of the premaxilla suggests that it belonged to a relatively large individual, but larger conspecific specimens

are known; for example, the length of the premaxilla, from the apex to the premaxillary foramen, in the rostrum of the holotype IRSNB M.1887 is 528 mm. However, the height of our specimen is especially important as compared to the measurements presented by Lambert (2005: table 5). This fossil is perfectly preserved, and displays no trace of abrasion or splitting of its outer cortical layers. Its lateral surface bears the imprint of a loose vascular network composed of branching canals 1.2 to 1.3 mm in diameter. These canals apparently originate from regularly spaced vascular pits (interval 6–8 mm) located along the suture between the maxilla and the premaxilla.

The origin of this fossil, discovered in the area of Antwerp during the second part of the nineteenth century, is somewhat imprecise, as for most remains of fossil beaked whales from this area. It might originate from the Antwerp sands (Lambert, 2005), dated from lower to middle Miocene (Louwye et al., 2000), considering that another specimen of *A. recurvirostris* was found in that member (Lambert, 2005). With a condylobasal length estimated to 960 mm for the holotype (the skull of this specimen is incomplete at its posterior extremity; Fig. 1(C)), *A. recurvirostris* ranks among the largest known fossil ziphid species.

### 2.2. Comparative sample

In order to dispose on a comparative element representing the generalized (or non-specialized) structure of the premaxillae in toothed whales, a section 1 cm thick including the maxilla and the premaxilla was sampled from the middle part (left side) of the rostrum of an adult male bottlenose dolphin, *Tursiops truncatus truncatus* (specimen from personal collection; skull length 521 mm). This species is a relatively large (up to 4 m), bulky coastal dolphin displaying the unspecialized rostrum features (Fig. 1(D)) that occurred in early odontocetes and prevail in most extant forms: a hollow mesorostral groove (in dry skulls) and a lack of apparent pachyostosis or osteosclerosis (Fordyce, 2002; Mead and Fordyce, 2009).

### 2.3. Technical processing of the samples

Once photographed and measured, the premaxilla IRSNB 3810-M. 2012 a-b was sectioned transversely into seven segments numbered I to VII, representing the various regions of this bone (Fig. 1(A)). In each of these fragments, one ground section 80–120- $\mu$ m thick, oriented perpendicular to the sagittal axis of the premaxilla made (sections numbered “s1” to “s6” in a proximo-distal direction). The sections were observed at low and medium microscope magnification, in natural and polarized transmitted light. Because a pronounced increase in bone compactness represents one of the most obvious specialized traits of many ziphid rostra, this characteristic was quantified precisely in *Aporotus*. Measurements of bone compactness (parameter C) were performed for each section in nine square fields 2.5  $\times$  2.5 mm for the premaxilla, and two fields 5  $\times$  5 mm for the maxilla. These fields were distributed evenly in the deep and peripheral regions of the sections, as

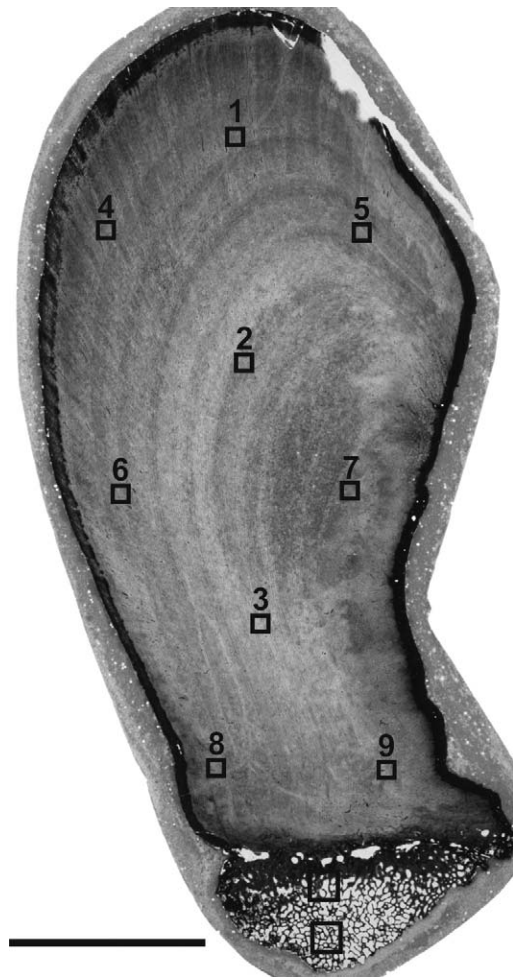


Fig. 2. Location of the fields used for compactness measurements in section 3. Fields are  $2.5 \times 2.5$  mm for the premaxilla, and  $5 \times 5$  mm for the maxilla.

shown on Fig. 2. All cavities more than  $10 \mu\text{m}$  in width or diameter were drawn via a microscope and a *camera lucida* (enlargement  $\times 80$ ). Their total area was then measured with the software Image J (Abramoff et al., 2004) and subtracted from the total area of the field to obtain the area actually occupied by the osseous tissue. The latter, expressed as a percent of the field area, gave a local compactness index ( $C_i$ ). The mean value of this index for the nine fields sampled in each section gave the value of parameter  $C$  for the whole section. The measurements of  $C$  made in the premaxilla, or  $C_p$ , were distinguished from the same measurements made in the maxilla, or  $C_m$ . Additional measurements (e.g., diameter of vascular canals) were made at higher magnification with a calibrated ocular micrometer.

Four transverse ground sections were made in the sample from the *Tursiops* premaxilla. In one of these sections, local compactness measurements ( $C_i$ ) were made in five local fields (Fig. 3), and parameter  $C_p$  was measured at once for the whole sectional area.

The terminology used in this study for describing the various types of osseous tissues refers to Francillon-Vieillot et al. (1990).

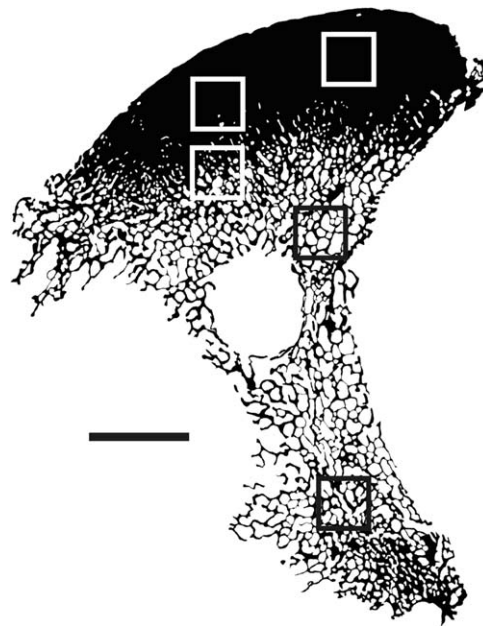


Fig. 3. General view of compactness distribution in *Tursiops truncatus* premaxilla, with indication of the five local fields ( $2.5 \times 2.5$  mm) used for measuring local bone compactness.

### 3. Results

#### 3.1. Microanatomical features of Aporotus premaxilla and maxilla

Whatever the location of the sections, the premaxilla displays a very high textural compactness (Figs. 2 and 4(A)), with  $C_p$  values from 96.8% to 98.8%. The only cavities occurring in this bone are vascular canals the diameters of which,  $16.5 \mu\text{m} \pm 4.5$  on average (extreme values: 10 and  $30 \mu\text{m}$ ), are very constant within each section, and between sections. There is no noticeable difference in bone compactness between the core (for this region:  $98.1\% < C_i < 98.6\%$  in all sections) and the peripheral layers ( $96.8\% < C_i < 98.8\%$ ) of the premaxilla cortex. Conversely, the maxilla is represented on this fossil by spongy bone displaying a loose texture, the compactness of which ranges from 65% (region edging the premaxilla) to 40–42% (core of the maxilla remnants).

The cortex of the premaxilla is entirely stratified by a succession of layers that alternatively display high and low opacity, and lay parallel to each other and to the outer contour of the bone (Fig. 4(A)). These layers correspond to cyclic growth marks. According to the definition proposed by Perrin and Myrick (1980), the association of a dark layer (supposed to represent fast sub-periosteal accretion) and a light layer (slower deposit), constitute a growth layer group, or GLG, the periodicity of which is considered basically annual (see also Klevezal, 1996; Castanet, 2006). Compactness differences neither occur between the dark and light layers of a single GLG, nor between the various GLGs of a single section. In the most developed part of the premaxilla (level of sections 2–4) there are eight well-characterized GLGs, and perhaps a 9th less sharp one (Fig. 4(A)); conversely, growth marks are too faint to be

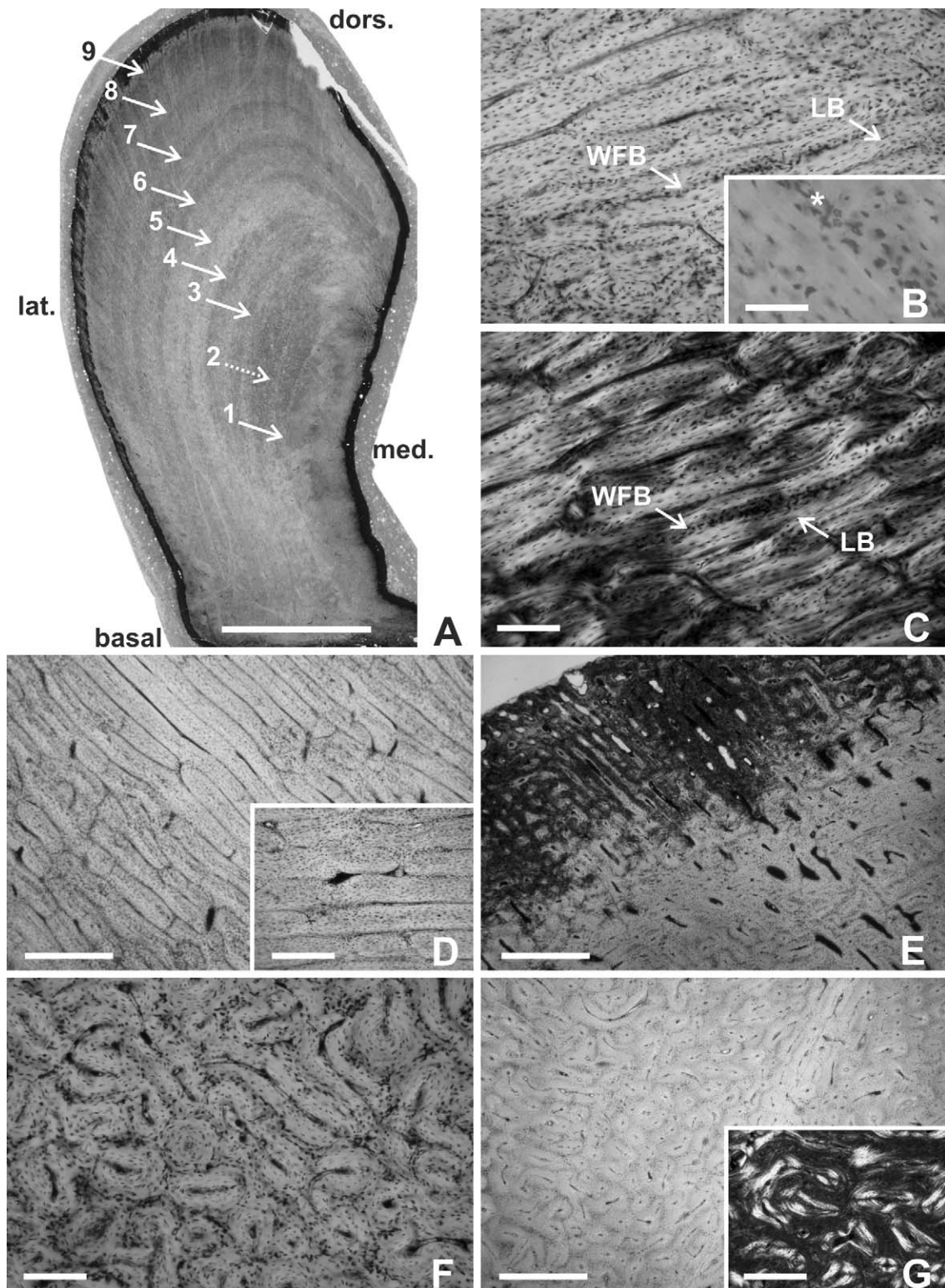


Fig. 4. Histology of *Aporotus* premaxilla. **A.** General structure of the bone in section 3. The bone is entirely compact with conspicuous, cyclic growth marks. The arrows and the numbers 1–9 indicate the GLGs, and their sequence of formation (1: earliest GLG). The second GLG (dotted arrow) is poorly characterized but nevertheless valid. **B.** Structure of the fibro-lamellar complex composing the premaxilla at medium (main frame) and higher (small frame) enlargements. **C.** Same field as for B, viewed in transmitted polarized light. Thin layers of mono-refringent woven-fibered bone (dark) are edged by birefringent deposits (bright) of lamellar bone tissue. **D.** Geometric structure of the laminar bone tissue at medium (main frame) and higher (small frame) enlargements. **E.** Radial primary osteons in the peripheral-most cortical layer in section 3. **F.** Reticular bone tissue in the deep layers of the premaxilla cortex. **G.** Fibro-lamellar complex with longitudinal osteons (cut transversely here) at the apex of the premaxilla (lower right corner: same tissue at higher magnification and in polarized light). Abbreviations and symbols: dors., dorsal surface of the premaxilla; lat., lateral surface; LB, lamellar bone; med., medial surface; WFB and asterisk, woven-fibered bone. Scale bars = 20 mm (A), 160  $\mu$ m (B main frame, C), 90  $\mu$ m (B small frame), 800  $\mu$ m (D main frame, E, G main frame), 450  $\mu$ m (D, G small frames).

counted in the most apical region of the bone (section 6). In the basal part of the premaxilla, GLG spacing is small but relatively constant from deep to superficial cortical regions. In the dorsal territory of the bone, GLG spacing is much broader, and shows a tendency to increase from deep to superficial cortical layers. GLG spacing directly reflects the local rate of sub-periosteal accretion during growth. Therefore, it can be inferred that the premaxilla grew faster in dorsal than in lateral direction, and that local growth speed in the dorsal region tended to increase in time, at least up to the ontogenetic stage that our specimen had reached. Due to intense remodeling, the maxilla remnants retain no primary bone tissue, and thus no trace of a cyclic growth pattern.

### 3.2. Histological features of *Aporotus* premaxilla

The premaxilla is entirely formed of a fibro-lamellar complex, a type of primary osseous tissue combining woven-fibered bone deposited by the periosteum, with lamellar bone of endosteal origin (Fig. 4(B, C)). The histological features typical of these two kinds of osseous tissues are unambiguously identifiable. Woven-fibered bone is mono-refringent in polarized light and includes numerous rounded osteocyte lacunae, randomly distributed in the bone matrix. Conversely, lamellar bone displays an alternate birefringence resulting from a more or less sharply characterized succession of thin lamellae alternatively dark and light (collagen fibers are oriented orthogonally from one lamella to another), and spindle-like or flat osteocyte lacunae oriented parallel to the lamellae (Fig. 4(B)). The woven-fibered tissue contributes but for a small part to bone volume in the premaxilla (layers of this tissue are most often less than 120  $\mu\text{m}$ ). In the middle region of the premaxilla (sections 2–4), the fibro-lamellar complex displays an extremely regular spatial organization of the so-called ‘laminar’ type in most of the bone volume (Fig. 4(D)). As is typical in laminar bone, vascular canals are mainly organized in circular layers parallel to the contour of the bone. They are surrounded by a thick wall of lamellar tissue to form broad primary osteons inserted between the thin deposits of woven-fibered bone. In the dorsal and dorso-lateral territories of the premaxilla, radially oriented primary osteons, increasing in number towards cortical periphery, occur (Fig. 4(E)); local primary deposits are thus of the ‘radiating’ type. There is a third type of vascular orientation restricted to a thin crescent-like zone (9–10% of sectional area) edging the medial surface of the bone. In this region, primary osteons are longitudinal, oblique or radial, thus creating a so-called ‘reticular’ pattern (Fig. 4(F)).

This basic structure, associating a core of pure laminar bone with peripheral radial osteons, and a small medial area of reticular tissue, prevails in the proximal two thirds of the premaxilla (sections 1–4). In section 5, the geometry of the vascular network is more complex, with layers of circular canals alternating in the cortex with layers of longitudinal canals. In the most apical region of the bone (section 6), vascular orientation becomes mainly longitudinal (Fig. 4(G)). In all parts of the premaxilla, the outer-most cortical layer (in a band some 1.2 mm thick below the bone surface) is more cancellous than the rest of the cortex (Fig. 4(E)). This aspect is

due to the local occurrence of incomplete primary osteons that retain a relatively large lumen. Conversely, the medial surface of the bone is bordered by compact tissue displaying signs of superficial resorption.

Histologically, the growth marks of the premaxilla are defined in sections 1–4 by a difference in opacity (Fig. 5(A)) due to the volume of osteocyte lacunae: the latter are slightly bigger and more rounded in the dark than in the light layer of each GLG. For this reason, the GLGs are better distinguished in the thickest sections, where a spatial summation of faint opacity differences makes the stratified organization of the cortex more perceptible. In section 5, growth marks display an additional feature, a periodic shift in osteonal orientation. The dark layers of the GLGs have a laminar structure, whereas in the light layers, osteons are oriented longitudinally (Fig. 5(B)). In section 6, growth marks are no longer discernible in ordinary transmitted light. Four GLGs are nevertheless revealed in polarized light by thin (ca. 500–600  $\mu\text{m}$ ) brightly birefringent layers of circular primary osteons (Fig. 5(C)).

In most of its volume, the premaxilla is void of Haversian remodeling. It is thus made of a primary bone deposit that clearly reflects the pattern and rate of cortical growth. The only place where some remodeling activity is noticeable is the most superficial zone of the crescent-like medial area, in which the bone tissue displays small diameter Haversian systems (Fig. 5(D)).

### 3.3. Histological features of *Aporotus* maxilla

Histologically, the maxilla is extremely different from the premaxilla, though these bones are closely sutured (Fig. 5(E–G)). The limit between them is marked by both a local concentration of wide vascular canals opening outside by pits (Fig. 5(E, F)), and by densely-packed secondary osteons created by Haversian remodeling (Fig. 5(G)). The trabeculae forming the spongiosa of the maxilla are intensely remodeled, and entirely made of thin endosteal platings of lamellar tissue separated by reversion lines (Fig. 5(H)). Such a trabecular structure is very common in spongy bone formations, be they of endosteal-endochondral origin (endochondral bones) or derived from the inner resorption of originally compact periosteal deposits (situation of the maxilla).

### 3.4. Microanatomy and histology of *Tursiops* premaxilla

The dorsal part of *Tursiops* premaxilla consists of a compact cortex (it occupies some 40% of whole sectional area) with a mean local compactness 96.2–97.1% (Fig. 3). This cortex obviously corresponds to the ‘porcellaneous’ part of the delphinid premaxillae mentioned by Mead and Fordyce (2009). The basal part of the premaxilla, edging the suture with the maxilla, is composed of a loose spongiosa 30.9–40.6% in compactness. Between these two regions, a narrow transition zone exhibits intermediary compactness (some 61.3%). The value of parameter Cp for the whole section is 52.1%. The maxilla is made of loose spongy bone in most of its area, with the exception for a more compact band bordering the palatal surface.

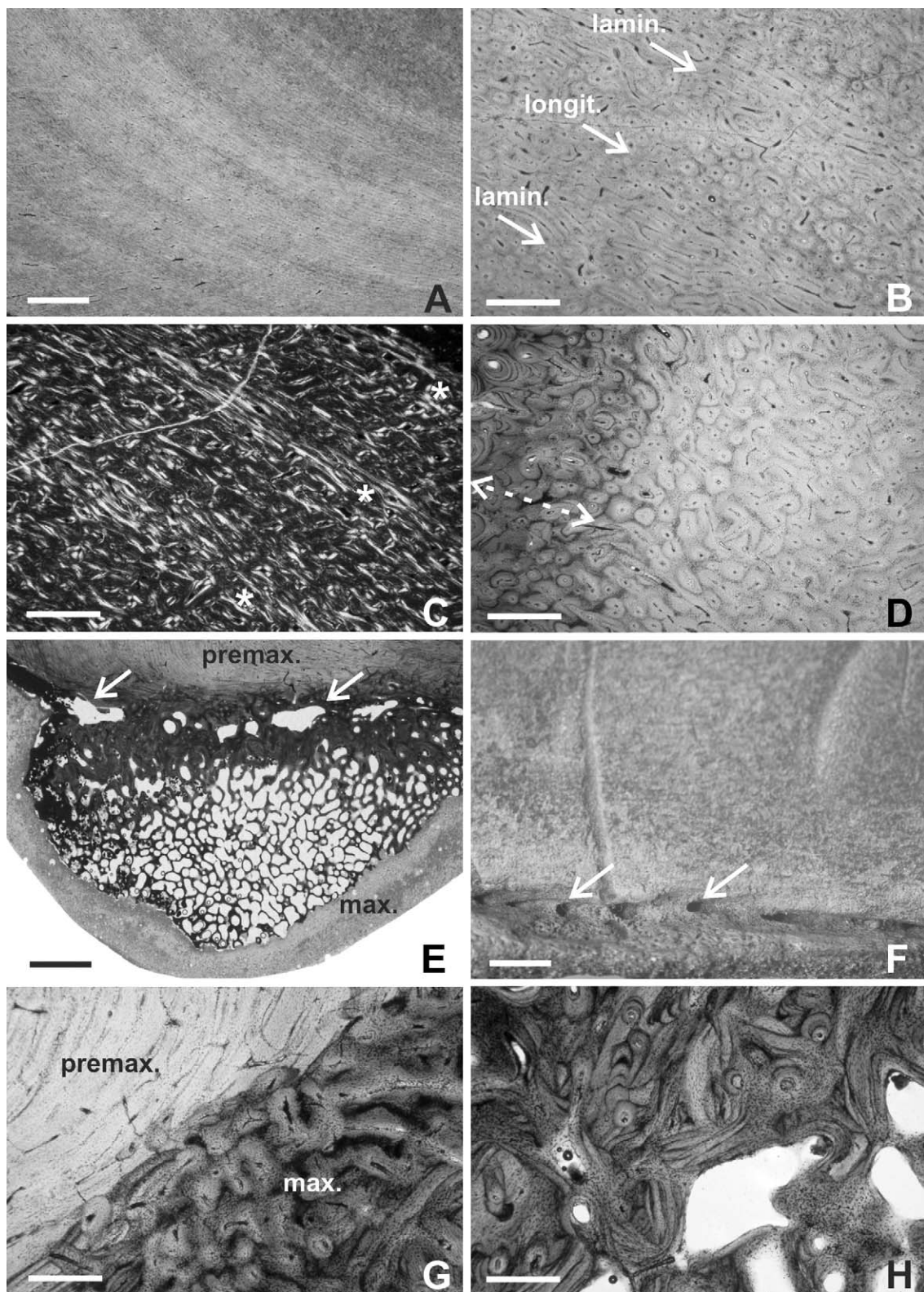


Fig. 5. Histology of *Aporotus* premaxilla and maxilla. **A.** Difference in opacity between the two layers forming the GLGs. **B.** Periodic difference in the orientation of primary osteons in section 5. **C.** Growth marks in section 6 as viewed in polarized light. **D.** Haversian remodeling in the deep cortex of the premaxilla. Secondary osteons are restricted to a narrow area along the medial face of the bone. **E.** Suture between the premaxilla and maxilla. **F.** Neuro-vascular pits opening outside the bone at the suture between premaxilla and maxilla. **G.** Haversian bone remodeling at the level of the suture between premaxilla and maxilla. **H.** Remodeled spongiosa forming most of the maxilla. Abbreviations and symbols: lamin., laminar bone; longit., fibro-lamellar complex with longitudinal primary osteons; max., maxilla; premax., premaxilla; arrows on Figs. E and F point at big vascular canals or pits; asterisks, layers of laminar bone tissue; dotted arrow, width of the narrow medial zone in which Haversian remodeling occurs. Scale bars = 4 mm (A), 800  $\mu$ m (B, C, D, G, H), 3.6 mm (E), 18.5 mm (F).

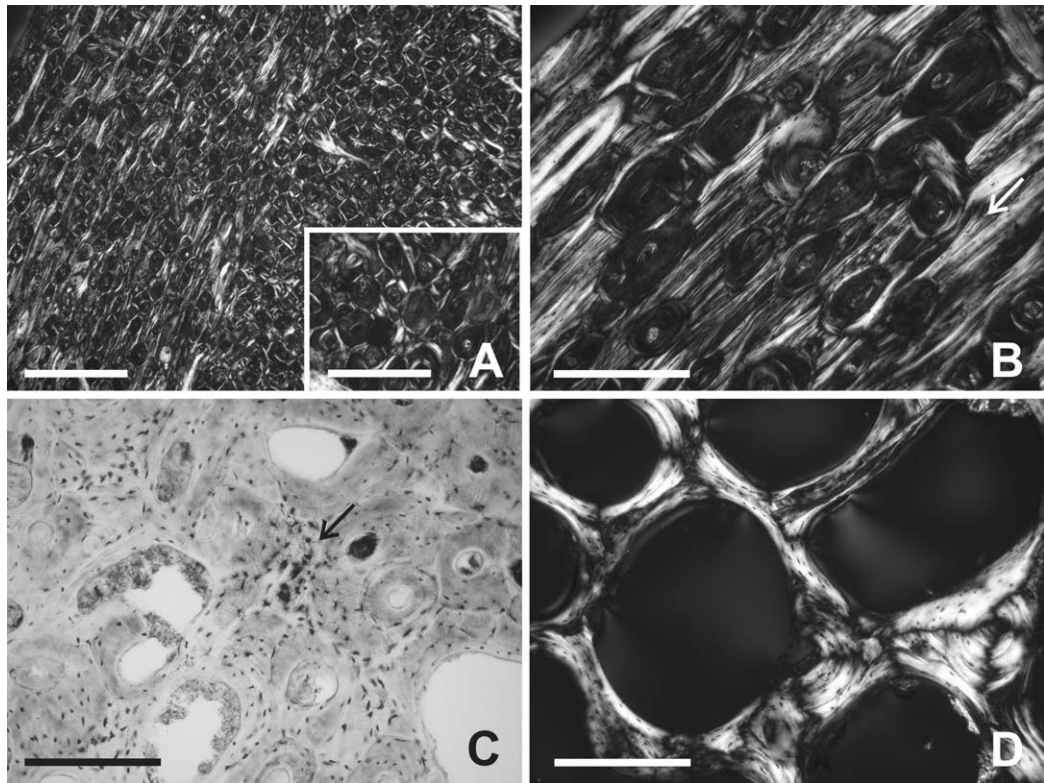


Fig. 6. Histology of *Tursiops truncatus* premaxilla. **A.** Remodeled compact cortex displaying typical secondary osteons (Havers' systems), with detailed view on dense Haversian tissue present in the deep cortex. **B.** Mildly remodeled peripheral cortex showing remnants of the thick layer of parallel-fibered tissue (arrow) deposited by the periosteum before growth ceased. **C.** Remnants of woven-fibered periosteal tissue (arrow) in the deep cortex. **D.** Intensely remodeled trabeculae forming the spongiosa of the premaxilla. Scale bars = 1 mm and 500 µm (A), 400 µm (B, C, D).

Histologically, the compact cortex of *Tursiops* premaxilla is made of a dense Haversian tissue created by the intense, sustained remodeling of the cortex (Fig. 6(A)). Secondary osteons are oriented longitudinally, and their walls are made of more or less typical lamellar tissue, a normal feature of Havers' systems in tetrapods. Remnants of primary bone tissue are sparse. In a broad peripheral area of the cortex (*ca.* one third of cortical thickness), where osteonal density is lesser, they consist of brightly birefringent lamellar or parallel-fibered bone (Fig. 6(B)). In the deep regions of the compact cortex, the few remnants of periosteal tissue are of the woven-fibered type (Fig. 6(C)). In the transition zone, the compact cortex undergoes an extensive process of imbalanced remodeling: the volume of bone tissue destroyed by resorption is not completely compensated by secondary accretion; as a consequence, the bone progressively turns from compact to cancellous. The trabeculae forming the deep spongiosa are intensely remodeled (Fig. 6(D)), and entirely composed of a complex patchwork of lamellar bone platings.

#### 4. Discussion

##### 4.1. Growth pattern of *Aporotus* premaxilla

The premaxilla is a typical membrane bone; it is thus initially formed by an intradermic concentration of mesenchymal cells, the secretion of which creates a bone nodule that

quickly acquires the structure of a diploe, with a compact peripheral cortex and a cancellous core (cf. e.g., Krstic, 1988; Karaplis, 2008). This structure is normally maintained during growth by a double mechanism:

- Superficial, centrifugal growth of the cortex due to subperiosteal apposition;
- Patchy resorption of deep cortical layers that turn from compact to spongy (action of endosteal osteoclasts).

As exemplified by *Tursiops truncatus*, this resorptive process extends to the whole basal region in the odontocete premaxilla, thus creating a 'half diploe' organization of this bone, with a cancellous basal region loosely sutured to the maxilla, and a compact outer (dorsal) cortex. In *Aporotus recurvirostris*, the growth of the premaxilla was only based on cortical apposition; inner bone resorption did not occur. As a consequence, this bone had a completely osteosclerotic-like structure. If not submitted to inner resorption (remodeling process), laminar bone generally displays high compactness, at least in its mature form, when primary osteons are fully developed (e.g., Buffrénil and Schoevaert, 1989; Francillon-Vieillot et al., 1990). Conversely in very young, fast growing animals, primary osteons are still incompletely developed in newly accreted periosteal bone, which can give a high porosity to local laminar deposits. In our specimen, uncompleted primary osteons occur only in the outer-most (mainly dorsal)

deposits of radiating bone, which still retained a sustained growth rate when this individual died.

The fibro-lamellar complex composing the premaxilla is very common among amniotes (whatever the clade to which they belong), especially in the long bones of taxa that have a high metabolism and a fast growth (Ricqlès, 1975; Ricqlès et al., 1991). According to Castanet et al. (1996, 2000), vascular orientation within fibro-lamellar tissues would be loosely related to accretion rate; however, as experimentally evidenced by Margerie et al. (2002, 2004), a close correlation exists between these parameters, with noticeable discrepancies between the different bones of a single species, and for the same bone between distinct species. A longitudinal orientation of primary osteons would thus reflect relatively moderate appositional rates, whereas a radial orientation would characterize the fastest bone deposits (up to 171  $\mu\text{m}$  per day in the humerus of the king penguin, *Aptenodytes patagonicus*). Mechanical stress could possibly also contribute to influencing vascular orientation (Margerie et al., 2004). Further documentation is, of course, needed to decipher the puzzle of vascular orientation determinisms, a question that proves to be complex (e.g., Klein et al., 2009). In the case of *Aporotus* premaxilla, the spectacular differences in vascular orientation that distinguish deep and more superficial cortical layers could hardly be explained by the hypothesis of contrasted mechanical constraints acting sequentially on this bone at various growth stages; therefore, a prominent influence for accretion speed remains the most plausible interpretation. In this respect, the spacing pattern of growth marks would confirm that a fibro-lamellar complex including radial canals is deposited at a higher rate than typical laminar tissue. In conclusion, histological observations converge to show that growth was very fast on the dorsal, and to lesser extent latero-dorsal surfaces of *Aporotus* premaxilla. Conversely, growth was slower on the lateral wall of this bone. Considering that the premaxilla used for this study was from a relatively large individual (see Section 2), the fast apposition that was still proceeding on the dorsal surface of this bone by the time the individual died obviously means that local periosteal accretion remained very active up to advanced developmental stages. A very different trend occurs in *Tursiops truncatus*: long before growth ceases, the bone deposited on the cortical surface of the premaxilla has already turned from the woven-fibered type to the parallel-fibered or the lamellar types, two kinds of osseous tissues resulting from a low appositional rate (less than 1.5  $\mu\text{m}/\text{day}$ ; Buffrénil and Pascal, 1984).

At the developmental stage that our specimen had reached, growth had stopped on the medial surface of the premaxilla to be replaced by the reverse process, i.e., extensive, superficial resorption. Therefore, the growth of *A. recurvirostris* premaxillae was off-centered, which resulted in a dorso-lateral drift of bone development. With reference to this growth geometry, the medial part of the premaxilla should be considered ontogenetically most ancient. The crescent-like, reticular layer covering the medial surface of the bone would thus represent a remnant of osseous tissue formed at a very early (fetal?) growth stage, subsequently remodeled by Haversian substitution, and

finally submitted to an extensive superficial resorption involved by growth drift.

In the course of ontogeny, the laminar tissue can develop in two different ways, depending on the taxon or skeletal region considered: it can either be submitted to active Haversian remodeling and be extensively replaced by secondary osteons, as in the long bones of many primates and carnivores, or remain void of extensive, inner remodeling throughout life, as in e.g., artiodactyl or dinosaur long bones (Currey, 2002). The latter situation was obviously that of *A. recurvirostris* premaxillae (with exception for the limited medial zone considered above), which is in marked contrast with the putative generalized condition represented by *Tursiops*. In *Aporotus*, sub-periosteal bone accretion presented feebly pronounced cyclic fluctuations resulting in the formation of GLGs. Such marks have also been observed on fracture surfaces in *Aporotus dicyrtus* and *Choneziphius planirostris*, two close relatives of *A. recurvirostris* (Lambert, 2005, pers. obs.). If these growth marks had indeed an annual periodicity, as in other tetrapods, then the specimen studied here died in the course of its 9th (eight GLGs) or 10th (nine GLGs) year. As compared to available data on age and growth in beaked whales, this age would correspond to a pre-adult or a young adult that might not have completed full somatic development, because somatic growth in the Ziphidae can proceed up to 15–20 years (cf. Perrin and Myrick, 1980; Mead, 1989).

The maxilla remnants are too fragmentary to allow a reconstruction of the growth pattern of this bone. They are composed of a strongly remodeled spongiosa, a feature totally opposite to the structure of the premaxilla. Remodeling of the maxilla is likely to have been imbalanced towards resorption (i.e., reconstruction deficit) because the histological features of the spongiosa suggest that it was formed from more compact cortical bone.

#### 4.2. Comparative elements

From anatomic, microanatomic and histological points of view, the premaxilla of *A. recurvirostris* differs strikingly from the rostrum of *Mesoplodon densirostris*. Their only common feature is an extremely high compactness index (98–99% in both cases). The most obvious difference between these two species is that only the premaxillae display a specialized structure in *Aporotus*, whereas all the bones forming the rostrum are touched in *M. densirostris* (rostral bones are intimately fused in this species, with a dominant role of the vomer in filling the mesorostral groove). Another conspicuous difference is the absence of pachyostosis in *M. densirostris* in the territory corresponding to the premaxillae (but osteosclerosis is extreme). A third difference revealed by the present study resides in the pattern of bone remodeling. There is nearly no remodeling in *Aporotus*, whereas the rostrum of *M. densirostris* is entirely composed of a very dense Haversian tissue the secondary osteons of which are all oriented parallel to the rostrum axis. The latter feature is reminiscent of the generalized condition displayed by *Tursiops truncatus*, although Havers' systems in *M. densirostris* have highly

atypical structural characteristics (see Section 1) that ultimately result in the exceptional mineral content of the rostrum in this species (more than 87%).

Of course, it is neither possible to assess in detail the condition of the collagenous meshwork of the *Aporotus* premaxilla, nor to estimate its mineralization rate. However, the histological observations presented above revealed no qualitative abnormality of the laminar tissue it is made of. In particular, most of its volume is occupied by highly birefringent lamellar bone, a tissue type known to have a high collagen content, but a relatively low (ca. 64–65%) mineralization rate (Francillon-Vieillot et al., 1990). It is thus very unlikely that *Aporotus* premaxillae presented the same ultrastructural peculiarities as those characterizing the osteons of *M. densirostris* rostrum.

With respect to the whole set of data and interpretations presented above, it can be concluded that, since the structural specializations of the rostrum in *Aporotus* and *M. densirostris* rely on quite distinct osteogenic mechanisms (intense Haversian remodeling *versus* lack of remodeling), in addition to bearing on different bone elements, and having different morphological results (osteosclerosis *versus* pachyosteosclerosis), they should not be considered as homologous, but rather convergent. This conclusion is further substantiated by the fact that, beyond the cases of *Aporotus recurvirostris* and *M. densirostris*, ziphiid whales display a spectacular diversity in the anatomical solutions they experienced for creating facial bony crests, protuberances, excrescences, or increasing local bone volume and compactness (e.g., Heyning, 1989; Lambert, 2005; Bianucci et al., 2007).

It nevertheless remains that the common trend of most ziphiid whales to increase bone mass or density in the rostral region of their skulls, by one mechanism or another, is a very peculiar feature that is likely to constitute the relevant solution to an original adaptive constraint common to the members of this family. In this respect, an apomorphic feature of the Ziphiidae could well reside in the ecological or functional trait that creates such a constraint, rather than in the phenotypic results induced by this selective pressure (for this question, see also Bianucci et al., 2007).

#### 4.3. Functional considerations

The functional role of the morphological and structural specializations of face bones in beaked whales remains poorly understood. Three main hypotheses, all speculative in the absence of experimental data, were proposed for the osteosclerosis of *M. densirostris* rostrum (critical review in MacLeod, 2002).

By “reinforcing” the rostrum, this feature (Heyning, 1984) would improve the efficiency of the head blows supposed to be given (but very seldom observed) by the tusk-bearing males during intraspecific fighting (Heyning, 1984; MacLeod, 2002; see also Lambert et al., 2010 for comments on fossil tusk-bearing beaked whales). This hypothesis is mainly supported by the sexual dimorphism that characterizes the distribution of high-density bones and mandibular tusks within extant ziphiid

species (e.g., Besharse, 1971), and by theoretical reconstructions of male combats (MacLeod, 2002). However it has to face a serious objection: dense, compact bones are prone to fast fracture propagation, and are thus poorly resistant to shock, especially if they are hypermineralized (Rogers and Ziopoulos, 1999; Ziopoulos et al., 2000; Currey, 2002). According to the results of the present study the structural characteristics of *Aporotus* premaxillae, though far from representing a mechanical optimum for impact loading, are somewhat less contradictory with the hypothesis of a mechanical reinforcement of the rostrum than the characteristics of *M. densirostris* rostrum. Recent studies (e.g., Heyning, 1989; Cranford et al., 2008) pointed out that the differences between the facial anatomy of male and female ziphiids are not limited to the shape or density of bones: they also extend to the organization and development of acoustically important fat masses (melon and anterior spermaceti organ), which suggests that differences in bone characteristics could actually be part of a more complex sexual dimorphism involving the acoustic behavior of males and females.

A slight increase in skull mass could have the effect of a ballast facilitating the maintenance of a vertical orientation of the body during the descent phase of the extremely deep dives (e.g., Hooker and Baird, 1999; Tyack et al., 2006; Baird et al., 2008) commonly performed by beaked whales (Buffrénil and Casinos, 1995). Our results confirm the occurrence of increased bone mass located at the apical extremity of the body in *Aporotus recurvirostris*; however they also suggest that, in such a large species (its total mass can be estimated to several tons by comparison with extant species of similar length), the relative mass increase of the premaxillae (some kilograms, at most) must have been negligible and of no perceptible effect on buoyancy, trim, or dynamic equilibrium in water.

Hard and stiff rostrum bones could possibly be involved in the intracranial transmission of vibration waves involved in echolocation (Buffrénil and Casinos, 1995; see also Ziopoulos et al., 2000). A recent, and much more explicit variant of this hypothesis considers that the high-density bones, forming the premaxillary basin that encases the fat masses through which emitted vibrations travel (especially the anterior spermaceti organ), would act as acoustic reflectors, or “waveguide”, able to focalize the vibration waves emitted by the animals (Cranford et al., 2008). Toothed whales adapted to shallow dives (majority of non-ziphiid species) use air-filled ducts as acoustic reflectors; conversely, deep divers (all ziphiids) are obliged to use a non-compressible tissue. Hard and dense osteosclerotic bones could therefore constitute the most efficient solution. The present study reveals that the histological organization of *A. recurvirostris* premaxillae, though by far less extreme than that of *M. densirostris* rostrum, is nevertheless indicative, at least, of high stiffness and density, two characteristics well-suited to Cranford et al.’s (2008) model. In this respect, the local variations of the inner structure of *Aporotus* premaxilla (vascular orientation, local remodeling, etc.) would be of no functional consequence because they do not bear on the stiffness, density and surface hardness of the bone.

In the present state of knowledge, this hypothesis is the sole that could be compatible with three sets of observations:

- The exclusive occurrence of high-density face bones in the ziphids, which are, together with the sperm whale *Physeter macrocephalus*, by far the deepest divers among extant cetaceans;
- The morphological diversity of osteosclerotic or pachyosteosclerotic face bones among ziphid taxa. This diversity could indeed correspond to discrepancies between species in, e.g., the morphology of their acoustically active fat masses, details of the use of their sonars, their foraging behaviors, etc.;
- The sexual dimorphism of face bones in ziphids; since it has been observed that there is also a dimorphism in the development of the melon and anterior spermaceti organ (Cranford et al., 2008).

Moreover, in the case of *Aporotus*, this interpretation would not be contradictory with, or exclusive of, a possible mechanical reinforcement of the rostrum.

## 5. Conclusion

In conclusion, the main information arising from this study is that rostrum densification can result from different osteogenic mechanisms in ziphid taxa, at least at a sub-family rank. At the level of morphogenetic processes (in addition to that of gross anatomy), this feature is thus a convergence, not a synapomorphy, between them. Conversely, the functional reason (i.e., selective pressure) why this feature evolved is likely to be common to all ziphid species, and would constitute an original characteristic shared by the members of this odontocete lineage. The multiplication of comparative studies on the structure of face bones (histology, ultrastructure, mineral content, mechanical behavior, etc.) should help assessing which interpretation, mechanical, acoustic, or a combination of the two, is the more plausible.

## Acknowledgements

We are grateful to M. Lemoine (Muséum national d'Histoire naturelle, Paris), for the making of the ground sections. We also thank E. Steurbaut and A. Folie (IRSNB, Department of Paleontology) for having accepted that the premaxilla IRSNB 3810-M. 2012 a-b be sacrificed for histology, and S. Berton (IRSNB, Department of Paleontology) for having performed the preliminary polished section of the specimen.

## References

Abramoff, M.D., Magalhães, P.J., Ram, S.J., 2004. Image processing with ImageJ. *Biophotonics International* 11, 36–42.

Baird, R.W., Webster, D.L., Schorr, G.S., McSweeney, D.J., Barlow, J., 2008. Diel variation in beaked whale diving behavior. *Marine Mammal Science* 24, 630–642.

Besharse, J.C., 1971. Maturity and sexual dimorphism in the skull, mandible, and teeth of the beaked whale, *Mesoplodon densirostris*. *Journal of Mammalogy* 52, 297–315.

Bianucci, G., Lambert, O., Post, K., 2007. A high diversity in fossil beaked whales (Mammalia, Odontoceti, Ziphidae) recovered by trawling from the sea floor off South Africa. *Geodiversitas* 29, 561–617.

Bianucci, G., Lambert, O., Post, K., 2010. High concentration of long-snouted beaked whales (genus *Messapicetus*) from the Miocene of Peru. *Palaeontology* 53, 1077–1098.

Buffrénil, V. de, Casinos, A., 1995. Observations histologiques sur le rostre de *Mesoplodon densirostris* (Mammalia, Cetacea, Ziphidae) : le tissu osseux le plus dense connu. *Annales des Sciences Naturelles, Zoologie* 16, 21–32.

Buffrénil, V. de, Pascal M., 1984. Croissance et morphogenèse postnatales de la mandibule du vison (*Mustela vison* Schreiber) : données sur la dynamique et l'interprétation fonctionnelle des dépôts osseux mandibulaires. *Canadian Journal of Zoology* 62, 2026–2037.

Buffrénil, V. de, Schoevaert, D., 1989. Données quantitatives et observations histologiques sur la pachystose du squelette du dugong, *Dugong dugon* (Müller) (Sirenia, Dugongidae). *Canadian Journal of Zoology* 67, 2107–2119.

Buffrénil, V. de, Zylberberg, L., Traub, W., Casinos, A., 2000. Structural and mechanical characteristics of the hyperdense bone of the rostrum of *Mesoplodon densirostris* (Cetacea, Ziphidae): summary of recent observations. *Historical Biology* 14, 57–65.

Castanet, J., 2006. Time recording in bone microstructures of endothermic animals. *Comptes Rendus Palevol* 5, 629–636.

Castanet, J., Curry-Rogers, K., Cubo, J., Boisard, J.J., 2000. Periosteal bone growth rates in extant ratites (ostrich and emu). Implications for assessing growth in dinosaurs. *Comptes Rendus de l'Académie des Sciences de Paris* 323, 543–550.

Castanet, J., Grandin, A., Abourachid, A., Ricqlès, A. de, 1996. Expression de la dynamique de la croissance dans la structure de l'os périostique chez *Anas platyrhynchos*. *Comptes Rendus de l'Académie des Sciences de Paris* 319, 301–308.

Cranford, T.W., McKenna, M.F., Soldevilla, M.S., Wiggins, S.M., Goldbogen, J.A., Shadwick, R.E., Krysl, P., St. Leger, J.A., Hildebrand, J.A., 2008. Anatomic Geometry of Sound Transmission and Reception in Cuvier's Beaked Whale (*Ziphius cavirostris*). *Anatomical Record* 291, 353–378.

Currey, J.D., 2002. *Bones: structure and mechanics*. Princeton University Press, Princeton.

Heyning, J.E., 1984. Functional morphology involved in intraspecific fighting of the beaked whale *Mesoplodon carlhubbsi*. *Canadian Journal of Zoology* 62, 1645–1654.

Heyning, J.E., 1989. Comparative facial anatomy of beaked whales (Ziphidae) and a systematic revision among the families of extant Odontoceti, County Museum Contributions in Science, Los Angeles, 406, 1–65.

Hooker, S.K., Baird, R.W., 1999. Deep diving behavior of the northern bottlenose whale, *Hyperoodon ampullatus* (Cetacea: Ziphidae). *Proceedings of the Royal Society of London B* 266, 671–676.

Fordyce, R.E., 2002. *Simocetus rayi* (Odontoceti: Simocetidae) (new species, new genus, new family), a bizarre new archaic Oligocene dolphin from the eastern North Pacific. *Smithsonian Contributions to Paleobiology* 93, 185–222.

Francillon-Vieillot, H., Buffrénil, V. de, Castanet, J., Géraudie, J., Meunier, F.J., Sire, J.Y., Zylberberg, L., Ricqlès, A. de, 1990. Microstructures and mineralization of vertebrate skeletal tissues. In: Carter, J. (Ed.), *Skeletal biomineralizations: patterns, processes and evolutionary trends* 1, Van Nostrand Reinhold, New York, pp. 471–530.

Karaplis, A.C., 2008. Embryonic development of bone and regulation of intramembranous and endochondral bone formation. In: Belezikian, J.P., Raisz, G., Martin, T.J. (Eds.), *Principles of bone biology*, vol. 1. Academic Press, Amsterdam, pp. 53–84.

Klein, N., Scheyer, T., Tütken, T., 2009. Skeletochronology and isotopic analysis of a captive individual of *Alligator mississippiensis* Daudin, 1802. *Fossil Record* 12, 121–131.

Klevezal, G.A., 1996. Recording structures of mammals: determination of age and reconstruction of life history. Balkema, Rotterdam.

Krstic, R.V., 1988. *Atlas d'histologie générale*. Éditions Masson, Paris.

Lambert, O., 2005. Systematics and phylogeny of the fossil beaked whales *Ziphirostrum* du Bas, 1868 and *Choneziphius* Duvernoy, 1851 (Mammalia, Ziphidae).

Cetacea, Odontoceti), from the Neogene of Antwerp (North Belgium). *Geodiversitas* 27, 443–497.

Lambert, O., Bianucci, G., Post, K., 2010. Tusk-bearing beaked whales from the Miocene of Peru: sexual dimorphism in fossil ziphiids? *Journal of Mammalogy* 91, 19–26.

Louwye, S., De Coninck, J., Verniers, J., 2000. Shallow marine lower and middle Miocene deposits at the southern margin of the North Sea Basin (Northern Belgium): dinoflagellate cyst biostratigraphy and depositional history. *Geological Magazine* 137, 381–394.

MacLeod, C.D., 2002. Possible functions of the ultradense bone in the rostrum of Blainville's beaked whale (*Mesoplodon densirostris*). *Canadian Journal of Zoology* 80, 178–184.

Margerie, E. de, Cubo, J., Castanet, J., 2002. Bone typology and growth rate: testing and quantifying "Amprino's rule" in the mallard (*Anas platyrhynchos*). *Comptes Rendus Biologies* 325, 221–230.

Margerie, E. de, Robin, J.P., Verrier, D., Cubo J., Groscolas, R., Castanet, J., 2004. Assessing a relationship between bone microstructure and growth rate: a fluorescent labeling study in the king penguin chick (*Aptenodytes patagonicus*). *Journal of Experimental Biology* 207, 869–879.

Mead, J.G., 1989. Bottlenose whales *Hyperoodon ampullatus* (Forster, 1770) and *Hyperoodon planifrons* (Flower, 1882). In: Ridgway, S.H., Harrison, R. (Eds.), *Handbook of marine mammals. River dolphins and the larger toothed whales*, vol. 4. Academic Press, London, pp. 321–348.

Mead, J.G., Fordyce, R.E., 2009. The therian skull: a lexicon with emphasis on the odontocetes. *Smithsonian Contributions to Zoology* 627, 1–248.

Perrin, W.E., Myrick, A.C., 1980. Report of the workshop. In: Perrin, W.E., Myrick, A.C. (Eds.), *Age determination in toothed whales and sirenians*. Reports of the International Whaling Commission (Special Issue 3), Cambridge, pp. 1–50.

Ricqlès, A. de, 1975. Recherches paléohistologiques sur les os longs des tétrapodes. VII : Sur la classification, la signification fonctionnelle et l'histoire des tissus osseux des Tétrapodes. Première partie : structures. *Annales de Paléontologie (Vertébrés)* 61, 51–129.

Ricqlès, A. de, Buffrénil, V. de, 2001. Bone histology, heterochronies and the return of tetrapods to life in water: where are we? In: Mazin, J.M., Buffrénil, V. de (Eds.), *Secondary adaptation of tetrapods to life in water*, Verlag Dr. Friedrich Pfeil, München, pp. 289–306.

Ricqlès, A. de, Meunier, F.J., Castanet, J., Francillon-Vieillot, H., 1991. Comparative microstructure of bone. In: Hall, B.K. (Ed.), *Bone*, vol. 3: *Bone matrix and bone specific products*, CRC Press, Boca Raton, pp. 1–78.

Rogers, K.D., Ziopoulos, P., 1999. The bone tissue of the rostrum of a *Mesoplodon densirostris* whale: a mammalian biomineral demonstrating extreme texture. *Journal of Materials Science Letters* 18, 651–654.

Tyack, P.L., Johnson, M., Aguilar Soto, N., Sturlese, A., Madsen, P.T., 2006. Extreme diving of beaked whales. *Journal of Experimental Biology* 209, 4238–4253.

Ziopoulos, P., Currey, J.D., Casinos, A., 2000. Exploring the effects of hypermineralization in bone tissue by using an extreme biological sample. *Connective Tissue Research* 41, 229–248.

Ziopoulos, P., Currey, J.D., Casinos, A., Buffrénil, V. de, 1997. Mechanical properties of the rostrum of the whale *Mesoplodon densirostris*, a remarkably dense bony tissue. *Journal of Zoology* 241, 725–737.

Zylberberg, L., Traub, V., Buffrénil, V. de, Alizard, F., Arad, T., Weiner, S., 1998. Rostrum of a toothed whale: ultrastructural study of a very dense bone. *Bone* 23, 241–247.